= 0.76 mm s^{-1}, DI = 0.35 mm s^{-1}. Anal. Calcd for $C_{37}H_{42}F_6FeP_3$: C, 59.29; H, 5.65. Found: C, 59.07; H, 5.77.

5PF$_6$. ^{1}H NMR (CH_2Cl_2, 298 K): 5.16 (*p*-H, Ph), 8.97 (*m*-H, Ph), 3.42 (*o*-H, Ph), -1.33 (P–CH_2–), -4.34 (OCH_3), -9.40 (CH_2O), -17.73 (C_5Me_5). ESR (THF, 133 K): *g* = 2.48, 2.03. Mössbauer (77 K, Fe): SQ = 0.95 mm s^{-1}, DI = 0.35 mm s^{-1}. Anal. Calcd for $C_{38}H_{44}F_6FeP_3$: C, 58.55; H, 5.69. Found: C, 58.23; H, 5.73.

7. **Synthesis of [Fe(C_5Me_5)(dppe)R]TCNQ (R = CH_3 (4TCNQ), R = CH_2OCH_3 (5TCNQ)).** To a 10-mL CH_2Cl_2 solution of 3 mmol of 4 (1.81 g) or 5 (1.90 g) at 20 °C was added 3 mmol (0.612 g) of TCNQ. The red solution immediately turned green, and after the mixture was stirred for 1 h, 100 mL of ether was added. A dark green salt was precipitated and then washed with ether. Green microcrystals were recovered in 75% (4TCNQ, 1.81 g) or 70% yield (5TCNQ, 1.88 g). 4TCNQ, Anal. Calcd for $C_{49}H_{46}FeN_4P_2$ (4TCNQ): C, 72.77; H, 5.73; N, 6.93. Found: C, 72.49; H, 5.88; N, 6.71. Calcd for $C_{50}H_{48}N_4FeOP_2$ (5TCNQ): C, 71.6; H, 5.77; N, 6.68. Found: C, 71.31; H, 5.63; N, 6.97.

Acknowledgment. We are grateful to J. E. Guerchais (Brest, France), F. Varret (Paris), and H. Noël for the ESR, Mössbauer, and magnetic measurement facilities. S. Sinbandhit (CRMPO, Rennes, France) is gratefully acknowledged for NMR assistance. We are also indebted to the Laboratoires Standa (Caen, France) for financial support to C.R.

Supplementary Material Available: For 1, complete tables of atomic coordinates and their estimated standard deviations, bond lengths and angles, and general temperature factor expressions (5 pages); a listing of observed and calculated structure factors (18 pages). Ordering information is given on any current masthead page.

A Ferracarborane Analogue to [Fp]$^-$. Synthesis and Reactions of [*closo*-3,3-$(CO)_2$-3,1,2-$FeC_2B_9H_{11}$]$^{2-}$

Sharon S. Lee, Carolyn B. Knobler, and M. Frederick Hawthorne*

Department of Chemistry and Biochemistry, University of California, Los Angeles, Los Angeles, California 90024

Received July 6, 1990

Reduction of [*closo*-3,3,3-$(CO)_3$-3,1,2-$FeC_2B_9H_{11}$] (1) with 2 equiv of sodium naphthalide affords the high-yield synthesis of a formal iron(0) ferracarborane dianion [*closo*-3,3-$(CO)_2$-3,1,2-$FeC_2B_9H_{11}$]$^{2-}$ (3), as monitored by ^{11}B NMR spectroscopy. Complex 3 serves as a nucleophile in a variety of alkylation, acylation, and metalation reactions to yield ferracarborane anions of the type [*closo*-3,3-$(CO)_2$-3-L-3,1,2-$FeC_2B_9H_{11}$]$^-$ (4, L = CH_3; 5, L = $CH_2C_6H_5$; 6, L = $COCH_3$; 7, L = SnC_6H_5). The molecular structure of [$N(C_2H_5)_4$][7] has been determined by X-ray diffraction techniques. Compound 7 crystallized in the triclinic space group $P\bar{1}$ with a = 11.209 (1) Å, b = 13.026 (1) Å, c = 13.595 (1) Å, α = 79.959 (3)°, β = 84.143 (3)°, γ = 66.060 (2)°, V = 1785 Å^3, and Z = 2. In situ reactions of 3 with allyl and methylallyl chloride followed by subsequent loss of CO induced by ultraviolet radiation, resulted in the isolation of the corresponding η^3-allyl derivatives, [*closo*-3-CO-3-(η^3-CH_2CRCH_2)-3,1,2-$FeC_2B_9H_{11}$]$^-$ (8, R = H; 9, R = CH_3). The structure of 8 as the PPN$^+$ salt was also elucidated by single-crystal X-ray diffraction and found to crystallize in the monoclinic space group $P2_1/m$ with a = 9.1250 (7) Å, b = 25.011 (2) Å, c = 18.517 (2) Å, β = 91.328 (3)°, V = 4225 Å^3, and Z = 4 (two crystallographically different half-anions and one cation in the asymmetric unit). Migratory insertion of alkyls was demonstrated in the preparation of [*closo*-3-CO-3-$COCH_3$-3-$P(CH_3)_3$-3,1,2-$FeC_2B_9H_{11}$]$^-$ (10) by heating 4 and excess $P(CH_3)_3$ in THF for 7 days at the reflux temperature. A single-crystal X-ray diffraction study of [PPN][10] is reported. Complex 10 crystallized in the triclinic space group $P\bar{1}$ with a = 10.086 (4) Å, b = 15.390 (6) Å, c = 17.027 (7) Å, α = 112.636 (8)°, β = 96.647 (8)°, γ = 100.206 (9)°, V = 2351 Å^3, and Z = 2. The closo 12-vertex icosahedral geometry composed of a polyhedral FeC_2B_9-d_6 framework and pseudooctahedral coordination exhibited by the iron atom are common structural features displayed by all three of the ferracarboranes that were characterized crystallographically.

Introduction

The derivative chemistry of the ubiquitous [(η^5-C_5H_5)$Fe(CO)_2$] moiety, also known as Fp, is extensively documented in the literature.[1] In view of the close structural and electronic similarities of the dicarbollide and the cyclopentadienyl ligands,[2] we have continued our ongoing investigation of ferracarborane chemistry by developing a route to the metallacarborane counterparts of these Fp derivatives.

Recently, we reported the synthesis and structural characterization of mononuclear iron(II) ferracarboranes[3] and also that of [*closo*-(η^6-C_6H_6)-3,1,2-$FeC_2B_9H_{11}$].[4] As an effort to expand the relatively unexplored family of metallacarboranes containing iron, we have synthesized a ferracarborane analogue of [Fp]$^-$, the very nucleophilic [*closo*-3,3-$(CO)_2$-3,1,2-$FeC_2B_9H_{11}$]$^{2-}$ (3). In addition, we have prepared a series of novel ferracarborane anions via the reaction of a variety of electrophiles with 3. We also report here the detailed accounts of the synthesis and the full spectroscopic and structural characterization of three

---

(1) Gmelin Handbook of Inorganic Chemistry, Organoiron Compounds, Series B, Vols. 14, 1989, 85–122.

(2) (a) Hawthorne, M. F.; Young, D. C.; Wegner, P. A. *J. Am. Chem. Soc.* **1965**, *87*, 1818. (b) Hawthorne, M. F.; Young, D. C.; Andrews, T. D.; Howe, D. V.; Pilling, R. L.; Pitts, A. D.; Reintjes, M.; Warren, L. F., Jr.; Wegner, P. A. *J. Am. Chem. Soc.* **1968**, *90*, 879. (c) Hawthorne, M. F. *Acc. Chem. Res.* **1968**, *1*, 28.

(3) Lee, S. S.; Knobler, C. B.; Hawthorne, M. F. *Organometallics*, in press.

(4) Lee, S. S.; Knobler, C. B.; Hawthorne, M. F. *J. Organomet. Chem.* **1990**, *394*, 29.

0276-7333/91/2310-1054$02.50/0

Scheme I

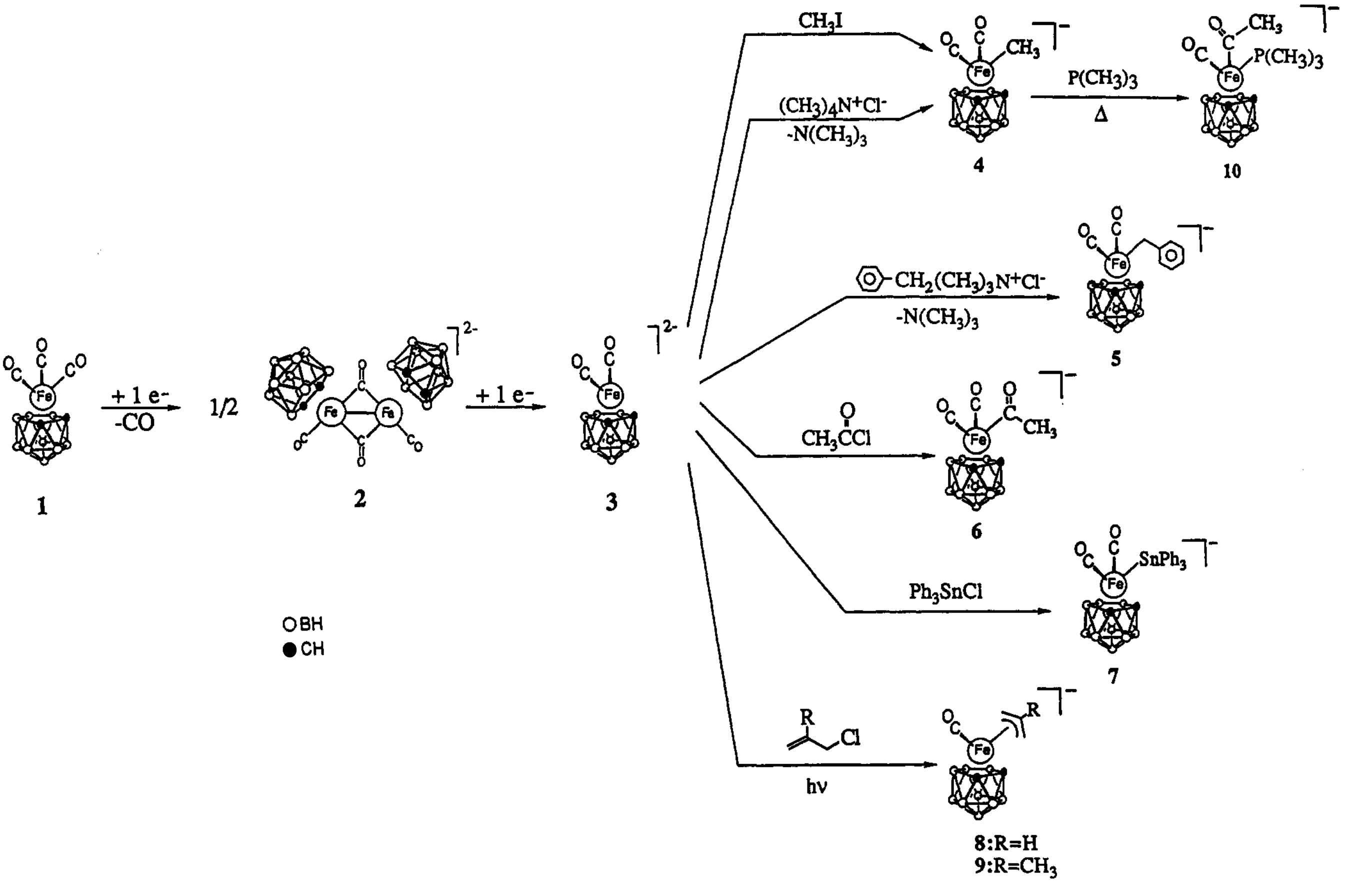

new ferracarboranes, which clearly demonstrate the versatility of **3** in synthesis.

Results and Discussion

Synthesis and Characterization of [*closo*-3,3-(CO)$_2$-3,1,2-FeC$_2$B$_9$H$_{11}$]$^{2-}$ (3). Since the reductive cleavage of [(η^5-C$_5$H$_5$)Fe(CO)$_2$]$_2$, Fp$_2$, to produce the reactive Fp anion is one of the most widely used reactions in transition-metal organometallic chemistry, a wide variety of reducing agents and reaction conditions have been investigated for this purpose.[5] Important aspects emphasized in this work included the need to avoid hazardous reagents, the elimination of side reactions, high yields, and convenience for subsequent in situ derivatization. Attempts to reduce the iron(I) dicarbollide dimer [*closo*-3-CO-3,3′-(μ-CO)-3,1,2-FeC$_2$B$_9$H$_{11}$]$_2^{2-}$ (**2**)[6] were carried out by using methodologies known to be effective for Fp$_2$ cleavage.

The sodium/mercury amalgam reduction of [N(CH$_3$)$_4$]$_2$[**2**] led to the isolation of the methylated dicarbonyl ferracarborane anion [*closo*-3,3-(CO)$_2$-3-CH$_3$-3,1,2-FeC$_2$B$_9$H$_{11}$]$^-$ (**4**) (vide infra) and not the expected iron(0) carborane analogue of [Fp]$^-$, [*closo*-3,3-(CO)$_2$-3,1,2-FeC$_2$B$_9$H$_{11}$]$^{2-}$ (**3**). Since the dianion **3** is expected to be highly nucleophilic compared to [Fp]$^-$, it was suspected that **4** results from the nucleophilic attack of the reduced species on the tetramethylammonium cation. This was substantiated by the identification of trimethylamine as a product of the reaction.

Unlike its cyclopentadienyl analogue, **2** is commercially unavailable and purification, regardless of the identity of the countercation, involves repeated fractional recrystallization, resulting in loss of material. This prompted a modification in the choice of starting material and led us to an extensive investigation of the two-electron reduction of the neutral iron(II) tricarbonyl derivative [*closo*-3,3,3-(CO)$_3$-3,1,2-FeC$_2$B$_9$H$_{11}$] (**1**)[3] to yield **3**.

From the wide array of reducing agents examined, we found that 2 equiv of sodium naphthalide rapidly and cleanly reduced **1** in THF at room temperature. The bright yellow solution of **1** in THF was titrated with a standardized sodium naphthalide solution and monitored by ^{11}B NMR spectroscopy. After the addition of 1 equiv of reductant, the ^{11}B{^{1}H} resonances at 11.2, −0.3, −3.4, −7.7, −14.6, and −18.8, representative of **1**, were no longer observed and a 1:1:2:2:2:1 pattern present at 1.2, −6.1, −8.3, −10.2, −19.9, and −22.4, indicated the formation of **2**. When an additional 1 equiv of sodium naphthalide/iron center was added, a six-line pattern at −10.9, −13.1, −15.1, −17.3, −25.2, and −27.6 supported the quantitative production of Na$_2$[**3**], as monitored by ^{11}B{^{1}H} NMR spectroscopy. The upfield shifts observed in the ^{11}B NMR spectrum, **1** < **2** < **3**, are consistent with the order of increasing electron density at the transition metal as mirrored in the formal oxidation states of the iron center.

Although **3** is extremely air and moisture sensitive, solutions of Na$_2$[**3**] in THF can be stored under nitrogen at room temperature for a period of 2 weeks with no apparent

---

(5) Reducing Agents for Fp$_2$: (a) Na amalgam (King, R. B. *Acc. Chem. Res.* **1970**, *3*, 417. (b) Sodium potassium alloy (Ellis, J. E.; Flom, E. A. *J. Organomet. Chem.* **1975**, *99*, 263). (c) Na dispersion (Reger, D. L.; Fauth, D. J.; Dukes, M. D. *Synth. React. Inorg. Met.-Org. Chem.* **1977**, *7*, 151). (d) Potassium hydride (Inkrott, K.; Goetze, R.; Shore, S. G. *J. Organomet. Chem.* **1978**, *154*, 1978). (e) Trialkylborohydrides (Gladysz, J. A.; Williams, G. M.; Tam, W.; Johnson, D. L.; Parker, D. W.; Selover, J. C. *Inorg. Chem.* **1979**, *18*, 553). (f) Sodium naphthalide (Gompper, K.; Bartmann, E. *Liebigs Ann. Chem.* **1980**, 229). (g) Potassium benzophenone ketyl (Plotkin, J. S.; Shore, S. G. *Inorg. Chem.* **1981**, *20*, 284). (h) Na sand (Bodnar, T.; Coman, E.; Menard, K.; Cutler, A. *Inorg. Chem.* **1982**, *21*, 1275). (i) Lithium naphthalide (Davies, S. G.; Simpson, S. J.; Thomas, S. E. *J. Organomet. Chem.* **1983**, *254*, C29).

(6) Ruhle, H. W.; Hawthorne, M. F. *Inorg. Chem.* **1969**, *8*, 176.

loss of purity. Attempts to isolate pure salts of **3** were frustrated by its highly nucleophilic and air-sensitive nature. Following the methodology frequently used in the identification of elusive nucleophilic anion species, the chemical identity of **3** was confirmed by in situ derivatization with electrophiles. As summarized in Scheme I, the preparation of alkyl, acyl, metal, and allyl derivatives of **3** proceeds smoothly in high yields, as determined by ^{11}B NMR analysis. These in situ reactions with **3** were conveniently conducted in the same Schlenk flask in which the dianion was prepared.

Syntheses and Characterizations of Species Derived from the Dicarbonylferracarborane Dianion. Since many elegant and useful transformations utilizing complexes of the type $[CpFe(CO)_2R]$ (where R = alkyl, allyl) have been reported,[7] it is of interest to prepare ferracarborane counterparts to [FpR].

Quantitative production of complex **4**, as observed by ^{11}B NMR spectroscopy, was obtained via the room-temperature methylation of Na_2[**3**], generated in THF, with methyl iodide. Complex **4** was also prepared in the anaerobic heterogeneous reaction of Na_2[**3**] with a slurry of $(CH_3)_4N^+Cl^-$ in acetonitrile. Unlike **3**, $[Fp]^-$ is unreactive toward tetramethylammonium chloride and has been isolated as the crystalline $(CH_3)_4N^+$ salt.[8]

The $^{11}B\{^1H\}$ FT NMR spectrum of **4**, showing relative area ratios of 1:1:2:2:2:1 is consistent with the icosahedral geometry found in other mononuclear ferracarboranes.[3] In the ^1H NMR spectrum, the two singlets observed at δ 2.15 and 0.14 in an intensity ratio of 2:3, are assigned to the carboranyl C–H and the methyl protons, respectively. The terminal carbonyl frequencies observed in the infrared spectrum of **4** are lower in comparison to those observed in the cyclopentadienyl counterpart, $FpCH_3$.[9] This is in good agreement with the greater M→CO back-bonding expected in **4**, which stems from an electron-enriched metal center that results from the presence of the dinegative and strongly electron donating dicarbollide ligand. Although **4** can be isolated in aqueous media, purification is best achieved by recrystallization using dry and deoxygenated solvents. In the solid state, a color change, indicative of air sensitivity, is observed after brief exposure to air.

The quarternary ammonium salt $C_6H_5CH_2(CH_3)_3N^+Cl^-$ is reported to react slowly with $[Fp]^-$, forming trimethylamine and $[FpCH_2C_6H_5]$.[8] The formation of trimethylamine also provided a pathway for the preparation of $[$*closo*-$3,3\text{-}(CO)_2\text{-}3\text{-}CH_2C_6H_5\text{-}3,1,2\text{-}FeC_2B_9H_{11}]^-$ (**5**) from the reaction of Na_2[**3**] with benzyltrimethylammonium chloride. Bright yellow crystals of **5** were isolated in high yield, and the PPN^+ (PPN = bis(triphenylphosphoranylidene)ammonium) salt of **5** showed no signs of decomposition in the solid state upon exposure to air.

The ion $[Fp]^-$ reacts with tetraphenylphosphonium chloride to yield [FpPh] and substantial amounts of Fp_2; yet PPN^+Cl^- was unreactive with $[Fp]^-$, leading to the isolation of [PPN][Fp].[8] Attempts to isolate $[PPN]^2$[**3**] via metathesis of PPN^+Cl^- and Na_2[**3**] was frustrated by the observed formation of the iron dimer, **2**.

Successful in situ acylation of **3** was carried out by using acetyl chloride to form $[$*closo*-$3,3\text{-}(CO)_2\text{-}3\text{-}COCH_3\text{-}3,1,2\text{-}FeC_2B_9H_{11}]^-$ (**6**), as confirmed by analytical and spectroscopic data. As in the case of $[N(CH_3)_4]$[**4**], $[(CH_3)P(C_6H_5)_3]$[**6**] shows signs of decomposition in the solid state after exposure to air for several hours. In the IR spectrum of **6**, the ν(C=O) frequency is observed at 1582 cm^{-1}. The ^{11}B and ^1H NMR spectra of $[(CH_3)P(C_6H_5)_3]$[**6**] were unexceptional in all respects.

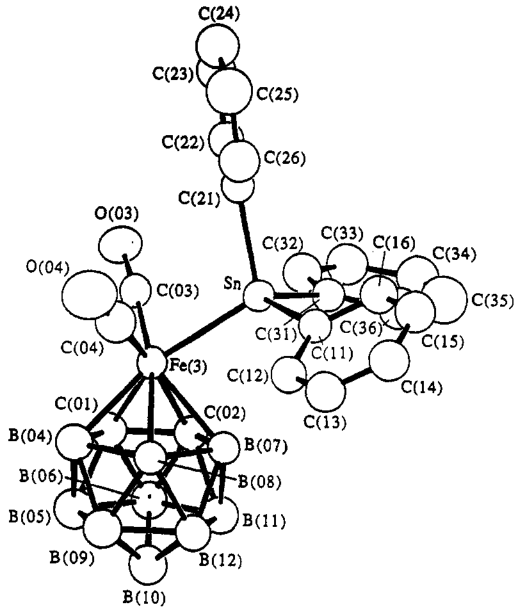

Figure 1. Structure of $[$*closo*-$3,3\text{-}(CO)_2\text{-}3\text{-}[Sn(C_6H_5)_3]\text{-}3,1,2\text{-}FeC_2B_9H_{11}]^-$ (**7**) in the $(C_2H_5)N^+$ salt showing the atom-labeling scheme. All hydrogen atoms have been omitted for clarity.

Attempts to synthesize the hydride complex $[$*closo*-$3,3\text{-}(CO)_2\text{-}3\text{-}H\text{-}3,1,2\text{-}FeC_2B_9H_{11}]^-$ via reactions of $[Na_2]$[**3**] with $(CH_3)_3N^+HCl^-$ or $[Na_2]$[**3**] with excess glacial acetic acid were unsuccessful, resulting only in the isolation of the ferracarborane dimer, **2**. The formation of Fp_2 via the corresponding formyl and hydride intermediates is well-known in FeCp chemistry.[10]

Following the recognition that the $AuPR_3$ fragment could form stable bonds to transition metals in a manner analogous to that established for the H ligand, a wide range of complexes have been synthesized from $(C_6H_5)_3AuCl$ and mononuclear metal carbonyl anions,[11] including $[FpAuP(C_6H_5)_3]$ and $[Fe(CO)_4(AuP(C_6H_5)_3)_2]$. When $[Na_2]$[**3**] in THF was reacted with triphenylphosphine gold chloride, the recently reported neutral ferracarborane $[$*closo*-$3,3\text{-}(CO)_2\text{-}3\text{-}P(C_6H_5)_3\text{-}3,1,2\text{-}FeC_2B_9H_{11}]$[3] was isolated. The precedence of the electron-transfer process over that of nucleophilic substitution is evident in the oxidation of **3** by Au^+. The similar oxidation chemistry of ferracarboranes by Cu^+ has been reported.[3]

Successful in situ metalations have been carried out with triphenyltin chloride and reactive metal carbonyl anions. Quantitative yields of the corresponding triphenyltin derivatives have been used as evidence in support of the effective reduction of transition-metal carbonyls to the corresponding anion.[5b] A THF solution of $[Na_2]$[**3**] was found to react with 1 equiv of triphenyltin chloride to produce $[$*closo*-$3,3\text{-}(CO)_2\text{-}3\text{-}Sn(C_6H_5)_3\text{-}3,1,2\text{-}FeC_2B_9H_{11}]^-$ (**7**). Orange crystals of $[N(C_2H_5)_4]$[**7**] are stable to prolonged exposure in air. As a complement to our synthetic studies, the molecular structure of $[N(C_2H_5)_4]$[**7**] was elucidated by single-crystal X-ray diffraction.

Structural Analysis of $[N(C_2H_5)_4]$[7]. The structure of **7** in the $(C_2H_5)_4N^+$ salt is shown in Figure 1. The ferracarborane-d_6 anion adopts a closo structure comprised

---

(7) Rosenblum, M. *Acc. Chem. Res.* **1974**, *7*, 122.

(8) Ellis, J. E. *J. Organomet. Chem.* **1976**, *111*, 331.

(9) (a) Piper, T. S.; Wilkinson, G. *J. Inorg. Nucl. Chem.* **1956**, *3*, 104. (b) King, R. B.; Bisnette, M. B. *J. Organomet. Chem.* **1964**, *2*, 15.

(10) Brown, D. A.; Glass, W. K.; Ubeid, M. T. *Inorg. Chim. Acta* **1984**, *89*, L47.

(11) Hall, K. P.; Mingos, D. M. P. *Prog. Inorg. Chem.* **1984**, *32*, 237 and references therein.

Table I. Selected Interatomic Distances and Angles for $[N(C_2H_5)_4][7]$

	Distances (Å)		
Sn–Fe(3)	2.554 (1)	Sn–C(11)	2.176 (2)
Sn–C(21)	2.186 (2)	Sn–C(31)	2.175 (2)
Fe(3)–C(03)	1.756 (3)	Fe(3)–C(04)	1.731 (4)
Fe(3)–C(01)	2.099 (3)	Fe(3)–C(02)	2.092 (3)
Fe(3)–B(04)	2.163 (4)	Fe(3)–B(07)	2.158 (3)
Fe(3)–B(08)	2.181 (4)	O(03)–C(03)	1.157 (4)
O(04)–C(04)	1.157 (5)	C(01)–C(02)	1.617 (4)
C(01)–B(04)	1.684 (5)	C(01)–B(05)	1.699 (5)
C(01)–B(06)	1.715 (5)	C(02)–B(06)	1.730 (5)
C(02)–B(07)	1.701 (4)	C(02)–B(11)	1.710 (4)
B(04)–B(05)	1.773 (6)	B(04)–B(08)	1.828 (5)
B(04)–B(09)	1.770 (5)	B(05)–B(06)	1.771 (6)
B(05)–B(09)	1.761 (6)	B(05)–B(10)	1.777 (6)
B(06)–B(10)	1.763 (6)	B(06)–B(11)	1.760 (5)
B(07)–B(08)	1.799 (5)	B(07)–B(11)	1.803 (5)
B(07)–B(12)	1.789 (5)	B(08)–B(09)	1.796 (5)
B(08)–B(12)	1.790 (5)	B(09)–B(10)	1.796 (6)
B(09)–B(12)	1.780 (5)	B(10)–B(11)	1.761 (6)
B(10)–B(12)	1.789 (6)	B(11)–B(12)	1.772 (6)
	Bond Angles (deg)		
Fe(3)–Sn–C(11)	118.1 (1)	Fe(3)–Sn–C(21)	112.5 (1)
Fe(3)–Sn–C(31)	110.4 (1)	C(11)–Sn–C(21)	101.8 (1)
C(11)–Sn–C(31)	108.5 (1)	C(21)–Sn–C(31)	104.5 (1)
Sn–Fe(3)–C(03)	83.0 (1)	Sn–Fe(3)–C(04)	85.6 (1)
Sn–Fe(3)–C(01)	143.6 (1)	Sn–Fe(3)–C(02)	100.2 (1)
Sn–Fe(3)–B(04)	158.4 (1)	Sn–Fe(3)–B(07)	80.6 (1)
Sn–Fe(3)–B(08)	108.8 (1)	C(03)–Fe(3)–C(04)	91.9 (2)
C(03)–Fe(3)–C(01)	91.4 (1)	C(03)–Fe(3)–C(02)	100.3 (1)
C(03)–Fe(3)–B(04)	118.2 (1)	C(03)–Fe(3)–B(07)	139.1 (1)
C(03)–Fe(3)–B(08)	167.8 (1)	C(04)–Fe(3)–C(01)	130.6 (1)
C(04)–Fe(3)–C(02)	167.0 (1)	C(04)–Fe(3)–B(04)	89.9 (2)
C(04)–Fe(3)–B(07)	123.6 (2)	C(04)–Fe(3)–B(08)	86.2 (2)
C(01)–Fe(3)–C(02)	45.4 (1)	C(01)–Fe(3)–B(04)	46.5 (1)
C(01)–Fe(3)–B(07)	80.5 (1)	C(01)–Fe(3)–B(08)	80.8 (1)
C(02)–Fe(3)–B(04)	80.4 (1)	C(02)–Fe(3)–B(07)	47.2 (1)
C(02)–Fe(3)–B(08)	80.9 (1)	B(04)–Fe(3)–B(07)	84.4 (1)
B(04)–Fe(3)–B(08)	49.8 (1)	B(07)–Fe(3)–B(08)	49.0 (1)
Fe(3)–C(03)–O(03)	176.2 (3)	Fe(3)–C(04)–O(04)	178.3 (3)
Fe(3)–C(01)–C(02)	67.1 (1)	Fe(3)–C(01)–B(04)	68.7 (2)
Fe(3)–C(01)–B(05)	126.8 (2)	Fe(3)–C(01)–B(06)	126.4 (2)
Fe(3)–C(02)–C(01)	67.6 (1)	Fe(3)–C(02)–B(06)	126.0 (2)
Fe(3)–C(02)–B(07)	68.5 (1)	Fe(3)–C(02)–B(11)	126.8 (2)
Fe(3)–B(04)–C(01)	64.8 (2)	Fe(3)–B(04)–B(05)	119.2 (2)
Fe(3)–B(04)–B(08)	65.6 (2)	Fe(3)–B(04)–B(09)	118.8 (2)
Fe(3)–B(07)–C(02)	64.4 (1)	Fe(3)–B(07)–B(08)	66.2 (2)
Fe(3)–B(07)–B(11)	118.2 (2)	Fe(3)–B(07)–B(12)	118.9 (2)
Fe(3)–B(08)–B(04)	64.6 (2)	Fe(3)–B(08)–B(07)	64.8 (2)
Fe(3)–B(08)–B(09)	116.7 (2)	Fe(3)–B(08)–B(12)	117.6 (2)
Sn–C(11)–C(12)	120.8 (1)	Sn–C(11)–C(16)	119.1 (1)
Sn–C(21)–C(22)	120.3 (1)	Sn–C(21)–C(26)	119.7 (1)
Sn–C(31)–C(32)	117.8 (1)	Sn–C(31)–C(36)	121.9 (2)

of the polyhedral FeC_2B_9 unit. The iron atom exhibits a pseudooctahedral coordination, with the dicarbollide ligand occupying three facial coordination sites and three monodentate ligands (two CO and one $SnPh_3$) occupying one site each. The C_2B_3 bonding face in 7 is essentially planar with no deviation from the least-squares plane by more than 0.016 (4) Å. The iron is approximately centered over the ring, giving rise to a Fe–C_2B_3 face (centroid) distance[12] of 1.557 Å. The Fe–Sn distance of 2.554 (1) Å in 7 is similar to that of 2.533 and 2.540 Å found in [FpSn$(C_6H_5)_3$].[13] Table I lists selected interatomic distances and angles for $[N(C_2H_5)_4][7]$. Overall, the bond lengths and bond angles within the carborane ligand are not unusual.

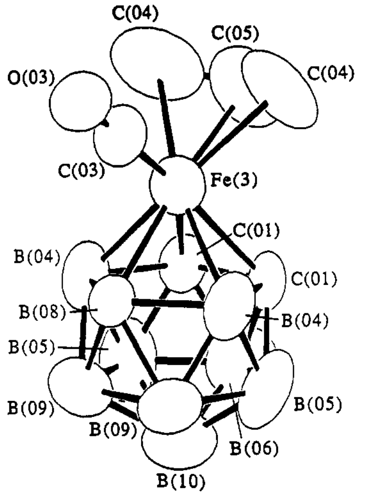

Figure 2. Structure of [*closo*-3-CO-3-(η^3-C_3H_5)-3,1,2-$FeC_2B_9H_{11}]^-$ (8) in the PPN^+ salt showing the atom-labeling scheme. All hydrogen atoms have been omitted for clarity. Due to the crystallographic mirror, the numbering scheme does not conform to nomenclature conventions.

Syntheses and Characterization of η^3-Allylferracarboranes. The reaction of $[Na_2][3]$ with allyl chloride followed by photolytically induced loss of CO, produced the 18-electron η^3-allyl complex [*closo*-3-CO-3-(η^3-C_3H_5)-3,1,2-$FeC_2B_9H_{11}]^-$ (8). Similarly, $[Na_2][3]$ reacted with methallyl chloride to produce the corresponding η^3-methallyl ferracarborane [*closo*-3-CO-3-(η^3-C_4H_7)-3,1,2-$FeC_2B_9H_{11}]^-$ (9). In the absence of ultraviolet irradiation, attempts to isolate the corresponding η^1-allyl ferracarborane only afforded the η^3-allyl complex in low yield. Although allyl acetate served as an electrophile with rhodacarborane anions,[14] $[Na_2][3]$ was unreactive toward allyl acetate. The formation of 8 must arise from a nucleophilic displacement reaction of 3 with allyl chloride to produce an η^1-intermediate that is unstable with respect to loss of CO. Photochemical ligand dissociation followed by a η^1 to η^3 rearrangement of the allyl fragment forms the observed product, 8.

The resonances observed in the 200-MHz ^1H NMR spectrum of [PPN][8] in CD_2Cl_2 were assigned on the basis of the assignments made in η^5-cyclopentadienyl (η^3-allyl) iron complexes.[15] The complex multiplet at δ 3.96 of relative area equivalent to one H was assigned to the methine proton (H_c) of the allyl ligand. The two syn protons (H_s) appear as a doublet ($J_{H_s-H_c}$ = 7 Hz), while the doublet ($J_{H_a-H_c}$ = 11 Hz) at δ 1.15 arises from the two anti protons (H_a). The characteristic broadness of the carboranyl C–H resonance was observed at δ 2.15 with a relative area equivalent to two H. The ^1H NMR spectrum of [PPN][9] exhibits comparable spectral features. Since no molecular structure for the cyclopentadienyl counterparts of 8 or 9 have been reported, an X-ray diffraction study of [PPN][8] was carried out.

Structural Analysis of [PPN][8]. Single crystals of [PPN][8] were grown by vapor diffusion of diethyl ether into an acetonitrile solution of the allyl ferracarborane.

---

(12) Fe–C_2B_3 plane distances: (a) 1.574 Å in $[(CO)_2P(C_6H_5)_3FeC_2B_9H_{11}]$, 1.545 Å in $[(CO)P(C_6H_5)_3(MeCN)FeC_2B_9H_{11}]$, 1.570 Å in $[(CO[P(OCH_3)_3]_2FeC_2B_9H_{11}]$, and 1.562 Å in $[(CO)_3FeC_2B_9H_{11}]$.[3] (b) 1.487 Å in $(C_6H_6)FeC_2B_9H_{11}$.[4] (c) 1.494 Å in $[(CH_3)C_6H_5]FeC_2B_9H_{11}$ and 1.480 Å in $[(CH_3)_2C_6H_4]FeC_2B_9H_{11}$ (Kang, H. C.; Knobler, C. B.; Hawthorne, M. F. *Inorg. Chem.* **1987**, *26*, 3409). (d) 1.480 Å in $[(CH_3)_3C_6H_3]FeC_2B_9H_{11}$ (Hanusa, T. P.; Huffman, J. C.; Todd, L. J. *Polyhedron* **1982**, *1*, 77). (e) 1.49 Å in $(C_5H_5)FeC_2B_9H_{11}$ (Zalkin, A.; Templeton, D. H.; Hopkins, T. E. *J. Am. Chem. Soc.* **1965**, *87*, 3988). (f) 1.58 Å in $Cs_2[(C_2B_9H_{11})_2Fe_2(CO)_4]\cdot(CH_3)_2CO\cdot H_2O$ (Greene, P. T.; Bryan, R. F. *Inorg. Chem.* **1970**, *9*, 1464).

(13) Bryan, R. F. *J. Chem. Soc. A* **1967**, 192. (No esd's were tabulated.)

(14) Walker, J. A.; Zheng, L.; Knobler, C. B.; Soto, J.; Hawthorne, M. F. *Inorg. Chem.* **1987**, *26*, 1608.

(15) Fish, R. W.; Giering, W. P.; Marten, D.; Rosenblum, M. *J. Organomet. Chem.* **1975**, *105*, 101.

Table II. Selected Interatomic Distances and Angles for [PPN][8][a]

	Distances (Å)		
C(01)–Fe(3)	2.081 (12)	C(01)–B(04)	1.711 (17)
C(01)–B(05)	1.69 (2)	C(01)–B(06)	1.71 (3)
C(01)–C(01)*	1.645 (16)	C(03)–O(03)	1.17 (2)
C(03)–Fe(3)	1.72 (2)	C(04)–C(05)	1.42 (2)
C(04)–Fe(3)	2.14 (2)	C(05)–Fe(3)	2.03 (3)
Fe(3)–B(04)	2.145 (14)	Fe(3)–B(08)	2.16 (2)
B(04)–B(05)	1.74 (2)	B(04)–B(08)	1.78 (2)
B(04)–B(09)	1.75 (2)	B(05)–B(06)	1.72 (2)
B(05)–B(09)	1.76 (2)	B(05)–B(10)	1.70 (2)
B(06)–B(10)	1.74 (4)	B(08)–B(09)	1.80 (2)
B(09)–B(10)	1.81 (3)	B(09)–B(09)*	1.77 (2)
	Bond Angles (deg)		
C(01)–Fe(3)–C(03)	151.2 (5)	C(01)–Fe(3)–C(04)	120.0 (6)
C(01)–Fe(3)–C(05)	90.5 (6)	C(01)–Fe(3)–B(04)	47.7 (5)
C(01)–Fe(3)–B(08)	82.9 (4)	C(01)–Fe(3)–C(01)*	46.5 (4)
C(01)–Fe(3)–C(04)*	93.1 (6)	C(01)–Fe(3)–B(04)*	81.4 (5)
C(03)–Fe(3)–C(04)	86.7 (6)	C(03)–Fe(3)–C(05)	106.9 (7)
C(03)–Fe(3)–B(04)	104.3 (5)	C(03)–Fe(3)–B(08)	80.3 (5)
C(04)–Fe(3)–C(05)	39.5 (7)	C(04)–Fe(3)–B(04)	166.1 (6)
C(04)–Fe(3)–B(08)	143.3 (6)	C(04)–Fe(3)–C(01)*	93.1 (6)
C(04)–Fe(3)–C(04)*	68.7 (7)	C(04)–Fe(3)–B(04)*	102.9 (6)
C(05)–Fe(3)–B(04)	127.3 (6)	C(05)–Fe(3)–B(08)	172.9 (6)
B(04)–Fe(3)–B(08)	49.0 (5)	B(04)–Fe(3)–C(01)*	81.4 (5)
B(04)–Fe(3)–C(04)*	102.9 (6)	B(04)–Fe(3)–B(04)*	82.8 (5)
C(01)*–Fe(3)–C(04)*	120.0 (6)	C(01)*–Fe(3)–B(04)*	47.7 (5)
C(04)*–Fe(3)–B(04)*	166.1 (6)	C(01)–B(04)–Fe(3)	64.2 (6)
Fe(3)–C(01)–B(04)	68.1 (6)	Fe(3)–C(01)–B(05)	123.7 (8)
Fe(3)–C(01)–B(06)	124.1 (8)	Fe(3)–C(01)–C(01)*	66.7 (6)
Fe(3)–B(04)–B(05)	117.4 (9)	Fe(3)–B(04)–B(08)	65.8 (6)
Fe(3)–B(04)–B(09)	120.2 (9)	Fe(3)–B(08)–B(04)	65.2 (6)
Fe(3)–B(08)–B(09)	117.3 (8)	C(05)–C(04)–Fe(3)	65.9 (10)
C(04)–C(05)–Fe(3)	74.6 (11)	C(04)–C(05)–C(04)*	117.5 (16)
O(03)–C(03)–Fe(3)	179.7 (10)		

[a] Positions marked by asterisks are related to tabulated positions by $x, {}^1/_2 - y, z$.

The asymmetric unit of the crystal has been shown to contain two crystallographically inequivalent anions, each with mirror symmetry. One of these anions is somewhat disordered in that the CO group lies near, rather than on, the mirror plane. The other independent anion, illustrated in Figure 2, displays the pseudooctahedral coordination exhibited by the iron in which two coordination sites are filled by the η^3-allyl ligand. As shown in the less disordered anion, cage atoms Fe(3), B(08), B(06), and B(10), carbonyl atoms C(03) and O(03), and the allyl carbon C(05), lie on the crystallographic mirror plane. This imposed crystallographic mirror is not uncommon in that it is also a structural characteristic of $[\eta^6\text{-}(C_6H_6)\text{-}3,1,2\text{-}FeC_2B_9H_{11}]$.[4] The C_2B_3 bonding faces for the ordered and disordered anions are planar (maximum deviation of 0.014 (15) and 0.020 (12) Å, respectively) with the iron approximately centered over the ring at distances of 1.530 (2) and 1.514 (2) Å, respectively, from the C_2B_3 plane.[12] Table II lists selected interatomic distances and angles for the less disordered anion found in the crystal structure of [PPN][8].

Synthesis of an Acylferracarborane via Alkyl Migration. The reaction of [Na][4] with trimethylphosphine in THF at the reflux temperature for 7 days produces $[closo\text{-}3\text{-}CO\text{-}3\text{-}COCH_3\text{-}3\text{-}P(CH_3)_3\text{-}3,1,2\text{-}FeC_2B_9H_{11}]^-$ (**10**). Although the acetyl derivative obtained from triphenylphosphine and [$FpCH_3$] was isolated in 72% yield after 60 h in refluxing THF,[5c] Na[4] was unreactive toward PPh_3 even after 7 days under these conditions.

The 160-MHz $^{11}B\{^1H\}$ FT NMR spectrum of **10** exhibited six peaks with the area ratio of 2:2:1:1:1:2, although a nine-line pattern is expected due to the asymmetry introduced by the chiral iron center. Most probably, coincidental overlaps of area equivalent to one H resonances are observed. The unsymmetrical nature of **10** is also demonstrated in the ^1H NMR spectrum, in which two broad singlets assigned to the nonequivalent carboranyl C–H vertices are observed at δ 1.92 and 1.41. The ^1H NMR spectra of the chiral ferracarborane $[closo\text{-}3\text{-}CO\text{-}3\text{-}(C_6H_5)_3\text{-}3\text{-}CH_3CN\text{-}3,1,2\text{-}FeC_2B_9H_{11}]^3$ also exhibit this spectral feature.

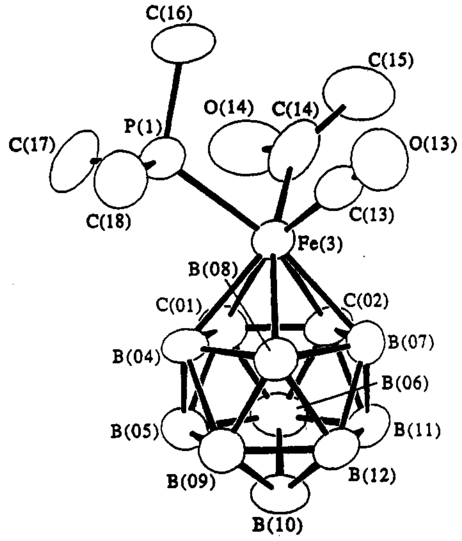

Figure 3. Structure of $[closo\text{-}3\text{-}CO\text{-}3\text{-}COCH_3\text{-}3\text{-}P(CH_3)_3\text{-}3,1,2\text{-}FeC_2B_9H_{11}]^-$ (**10**) in the PPN^+ salt showing the atom-labeling scheme. All hydrogen atoms have been omitted for clarity.

Since the structural information regarding the spatial orientation of various π-bonding ligands in metal acyl complexes has stimulated the search of an understanding of conformational properties,[16] an accurate structural analysis of [PPN][10] was sought.

Structural Analysis of [PPN][10]. The structure of [PPN][10], shown in Figure 3, displays three monodentate ligands and one $C_2B_9H_{11}$ unit, which occupies three facial coordination sites around the iron atom. Although a racemic mixture is found in the unit cell, the structure of one enantiomeric form of **10** is illustrated. The iron atom bonds symmetrically to the upper belt of the carborane cage with a Fe–C_2B_3 face (centroid) distance[12] of 1.572 (1) Å. The C_2B_3 bonding face is essentially planar with a maximum deviation of 0.018 (11) Å. The Fe–P distance of 2.188 (3) Å in **10** is similar to those of other chiral metal acyl complexes, e.g. 2.202 (2) Å in $[(\eta^5\text{-}C_5H_5)Fe(CO)(COCH_3)(P(C_6H_5)_3)]^{17}$ and 2.195 (2) Å in $[(\eta^5\text{-}CH_3C_5H_4)Fe(CO)(COCH_3)(P(C_6H_5)_3)]$.[17]

As found in other chiral metal acyl complexes,[17] the alignment of the acyl oxygen in **10** is also oriented antiperiplanar to the π-bonding CO. This is noteworthy because syn–anti conformational preferences cannot be adequately rationalized by considerations of steric interactions alone.[16] Although the torsion angle between the acetyl carbonyl and that of the π-bonding CO is found theoretically from extended Huckel and ab initio SCF MO calculations to be 0°,[18] the torsion angle of 14° found in [PPN][10] appears to be at variance with this theoretical value. Torsion angles of 18° in $[(\eta^5\text{-}C_5H_5)Fe(CO)(COCH_3)(P(C_6H_5)_3)]^{17}$ and 22° in $[(\eta^5\text{-}CH_3C_5H_4)Fe(CO)(COCH_3)(P(C_6H_5)_3)]^{17}$ are similarly in disagreement with the calculated angle. Table III lists the selected intera-

---

(16) Shambayati, S.; Crowe, W. E.; Schreiber, S. L. *Angew. Chem., Int. Ed. Engl.* **1990**, *29*, 256.

(17) Liu, H. Y.; Koh, L. L.; Eriks, K.; Giering, W. P.; Prock, A. *Acta Crystallogr.* **1990**, *C46*, 51.

(18) Davies, S. G.; Seeman, J. I.; Williams, I. H. *Tetrahedron Lett.* **1986**, *27*, 619.

Table III. Selected Interatomic Distances and Angles for [PPN][10]

	Distances (Å)		
Fe(3)–C(01)	2.090 (09)	Fe(3)–C(02)	2.101 (09)
Fe(3)–B(04)	2.148 (10)	Fe(3)–B(07)	2.147 (10)
Fe(3)–B(08)	2.203 (10)	Fe(3)–C(13)	1.757 (11)
Fe(3)–C(14)	1.974 (13)	Fe(3)–P(01)	2.188 (03)
C(01)–C(02)	1.630 (13)	C(01)–B(04)	1.713 (14)
C(01)–B(05)	1.712 (14)	C(01)–B(06)	1.732 (15)
C(02)–B(06)	1.727 (15)	C(02)–B(07)	1.658 (14)
C(02)–B(11)	1.692 (14)	B(04)–B(05)	1.800 (16)
B(04)–B(08)	1.731 (15)	B(04)–B(09)	1.757 (15)
B(05)–B(06)	1.791 (16)	B(05)–B(09)	1.773 (16)
B(05)–B(10)	1.775 (16)	B(06)–B(10)	1.767 (16)
B(06)–B(11)	1.733 (16)	B(07)–B(08)	1.789 (15)
B(07)–B(11)	1.768 (16)	B(07)–B(12)	1.766 (15)
B(08)–B(09)	1.762 (15)	B(08)–B(12)	1.775 (15)
B(09)–B(10)	1.786 (16)	B(09)–B(12)	1.758 (15)
B(10)–B(11)	1.770 (15)	B(10)–B(12)	1.792 (16)
B(11)–B(12)	1.769 (16)	C(13)–O(13)	1.085 (14)
O(14)–C(14)	1.207 (15)	P(03)–C(71)	1.782 (07)
C(14)–C(15)	1.370 (20)	P(01)–C(16)	1.817 (12)
P(01)–C(17)	1.817 (11)	P(01)–C(18)	1.820 (11)
	Bond Angles (deg)		
C(01)–Fe(3)–C(02)	45.8 (3)	C(01)–Fe(3)–B(04)	47.7 (4)
C(01)–Fe(3)–B(07)	79.1 (4)	C(01)–Fe(3)–B(08)	79.7 (4)
C(01)–Fe(3)–C(13)	163.4 (4)	C(01)–Fe(3)–C(14)	93.4 (4)
C(01)–Fe(3)–P(01)	105.3 (3)	C(02)–Fe(3)–B(04)	80.6 (4)
C(02)–Fe(3)–B(07)	45.9 (4)	C(02)–Fe(3)–B(08)	80.1 (4)
C(02)–Fe(3)–C(13)	119.5 (4)	C(02)–Fe(3)–C(14)	85.2 (4)
C(02)–Fe(3)–P(01)	148.6 (3)	B(04)–Fe(3)–B(07)	81.7 (4)
B(04)–Fe(3)–B(08)	46.9 (4)	B(04)–Fe(3)–C(13)	131.5 (5)
B(04)–Fe(3)–C(14)	135.0 (4)	B(04)–Fe(3)–P(01)	85.5 (3)
B(07)–Fe(3)–B(08)	48.5 (4)	B(07)–Fe(3)–C(13)	84.4 (5)
B(07)–Fe(3)–C(14)	116.8 (4)	B(07)–Fe(3)–P(01)	157.7 (3)
B(08)–Fe(3)–C(13)	90.6 (4)	B(08)–Fe(3)–C(14)	164.6 (4)
B(08)–Fe(3)–P(01)	110.0 (3)	C(13)–Fe(3)–C(14)	92.5 (5)
C(13)–Fe(3)–P(01)	90.7 (4)	C(14)–Fe(3)–P(01)	85.0 (4)
Fe(3)–C(13)–O(13)	176.1 (10)	Fe(3)–C(14)–C(15)	126.5 (9)
Fe(3)–C(14)–O(14)	118.9 (9)	O(14)–C(14)–C(15)	114.4 (11)
Fe(3)–P(01)–C(16)	116.2 (4)	Fe(3)–P(01)–C(17)	114.8 (4)
Fe(3)–P(01)–C(18)	115.4 (4)	C(16)–P(01)–C(17)	102.2 (5)
C(16)–P(01)–C(18)	100.4 (5)	C(17)–P(01)–C(18)	106.0 (5)
Fe(3)–C(01)–C(02)	67.5 (4)	Fe(3)–C(01)–B(04)	67.9 (5)
Fe(3)–C(01)–B(05)	127.1 (6)	Fe(3)–C(01)–B(06)	126.2 (6)
Fe(3)–C(02)–C(01)	66.7 (4)	Fe(3)–C(02)–B(06)	125.8 (6)
Fe(3)–C(02)–B(07)	68.5 (5)	Fe(3)–C(02)–B(11)	126.9 (6)
Fe(3)–B(04)–C(01)	64.4 (5)	Fe(3)–B(04)–B(05)	119.1 (6)
Fe(3)–B(04)–B(08)	68.2 (5)	Fe(3)–B(04)–B(09)	121.6 (6)
Fe(3)–B(07)–C(02)	65.6 (5)	Fe(3)–B(07)–B(08)	67.4 (5)
Fe(3)–B(07)–B(11)	120.2 (7)	Fe(3)–B(07)–B(12)	121.0 (7)
Fe(3)–B(08)–B(04)	64.9 (5)	Fe(3)–B(08)–B(07)	64.1 (5)
Fe(3)–B(08)–B(09)	118.5 (6)	Fe(3)–B(08)–B(12)	117.7 (6)

tomic distances and angles for [PPN][**10**].

Experimental Section

All manipulations were carried out under an atmosphere of argon by employing standard Schlenk techniques[19] or a Vacuum Atmospheres inert-atmosphere glovebox. All solvents were reagent grade and distilled from appropriate drying agents.[20] The following chemicals were purchased from the Aldrich Chemical Co. Naphthalene, methyl iodide, and acetyl chloride (gold label) were used as received. After opening, triphenyltin chloride was stored in the glovebox. Allyl chloride and methallyl chloride were distilled from calcium chloride prior to use. Alkyl ammonium chlorides (tetramethyl, tetraethyl, and benzyltrimethyl) were recrystallized from ethanol/ether and dried over P_2O_5. Bis(triphenylphosphoranylidene)ammonium chloride ((PPN)Cl) and methyltriphenylphosphonium bromide were purified from solutions of methylene chloride/ether and acetonitrile/ether, respectively. [*closo*-3,3,3-(CO)$_3$-3,1,2-FeC$_2$B$_9$H$_{11}$] (**1**)[3] was prepared according to literature methods.

Photochemical experiments were carried out by using a Hanovia 550-W medium-pressure mercury lamp. Solutions to be irradiated were placed in Pyrex Schlenk tubes supported 10 cm away from the light source.

^{1}H FT NMR spectra were obtained on a Bruker AF-200 spectrometer at 200.133 MHz. ^{11}B NMR spectra were recorded on a Bruker AM-500 FT-NMR (160.463 MHz) spectrometer. Proton and boron chemical shifts were referenced to residual solvent protons (CD_2Cl_2, 5.32 ppm) and external $BF_3{\cdot}OEt_2$, respectively. All chemical shifts downfield of the reference are designated as positive. Infrared spectra were recorded as Nujol mulls (NaCl) on a Beckman FT-1100 instrument. Elemental analyses were performed by Analytische Laboratorien, Gummersbach, FRG.

[Na$_2$][*closo*-3,3-(CO)$_2$-3,1,2-FeC$_2$B$_9$H$_{11}$] (3). General Procedure. A bright yellow solution of **1** (200 mg, 0.74 mmol) in 20 mL of THF was stirred during the dropwise addition of a deep green solution of sodium naphthalide, generated by stirring naphthalene (190 mg, 1.48 mmol) and excess sodium metal (100 mg, 4.35 mmol) in 40 mL of THF for 48 h at room temperature. After the excess sodium was washed twice with THF, the combined filtrates were added to the reaction. The resulting orange solution gave evidence for the quantitative production of Na$_2$[**3**], as monitored by ^{11}B NMR spectroscopy. ^{11}B{^{1}H} NMR (ppm, THF): −10.9, −13.1, −15.1, −17.3, −25.2, −27.6 (1:1:2:2:2:1).

[N(CH$_3$)$_4$][*closo*-3,3-(CO)$_2$-3-CH$_3$-3,1,2-FeC$_2$B$_9$H$_{11}$] (4). An orange solution of Na$_2$[**3**] generated from **1** (500 mg, 1.84 mmol) and 2 molar equiv of sodium naphthalide as described in the above general procedure was reacted with 0.12 mL of methyl iodide (2.0 mmol), resulting in an immediate color change to golden brown. The reaction was stirred at room temperature for 1 h followed by the removal of solvent. The residue was dissolved in 50 mL of degassed water, and aqueous $(CH_3)_4N^+Cl^-$ (210 mg, 1.92 mmol) was added. After filtration, the yellow precipitate was washed with water and diethyl ether, dried under vacuum, and recrystallized twice from CH_2Cl_2/heptane to afford an analytically pure product in a yield of 41% (252 mg). Anal. Calcd for $C_9H_{26}B_9NO_2Fe$: C, 32.41; H, 7.87; B, 29.17; N, 4.20; Fe, 16.75. Found: C, 32.26; H, 7.73; B, 28.91; N, 4.02; Fe, 16.50. IR (cm^{-1}): 2518, 2542 (B—H), 1992, 1913 (MC≡O). ^{1}H NMR (ppm, CD_2Cl_2): 3.22 (s, 12 H, N(CH$_3$)$_4$), 2.15 (br s, 2 H, carborane C—H), 0.14 (s, 3 H, –CH$_3$). ^{11}B{^{1}H} NMR (ppm, THF): −5.6, −7.2, −10.2, −11.7, −21.3, −23.1 (1:1:2:2:2:1).

An alternate route to [N(CH$_3$)$_4$][**4**] consists of adding a slurry of $(CH_3)_4N^+Cl^-$ (162 mg, 1.48 mmol) in 40 mL of acetonitrile to a solution of Na$_2$[**3**] (0.74 mmol) in THF. After stirring for 2 days, the solution was filtered over a Celite pad. Upon removal of solvent, the yellow residue was recrystallized twice from CH_2Cl_2/heptane to yield 120 mg of [N(CH$_3$)$_4$][**4**] (49% yield).

[PPN][*closo*-3,3-(CO)$_2$-3-C$_6$H$_5$CH$_2$-3,1,2-FeC$_2$B$_9$H$_{11}$] (5). A solution of [Na$_2$][**3**] (0.74 mmol) in THF was reacted with a slurry of benzyltrimethylammonium chloride (272 mg, 1.48 mmol) in 40 mL of THF, resulting in a color change to light yellow. The reaction was allowed to stir at room temperature for 24 h, followed by cannula filtration and removal of solvent. The yellow residue was dissolved in 40 mL of CH_3CN, and PPN$^+$Cl$^-$ (450 mg, 0.78 mmol) in CH_3CN (40 mL) was added. After filtration over a Celite pad, the yellow solution was reduced in volume and addition of diethyl ether afforded 523 mg (81%) of analytically pure product. Anal. Calcd for $C_{47}H_{48}B_9NO_2P_2Fe$: C, 64.58; H, 5.55; B, 11.13; N, 1.60; P, 7.09; Fe, 6.39. Found: C, 64.49; H, 5.40; B, 11.12; N, 1.46; P, 7.21; Fe, 6.29. IR (cm^{-1}): 2555, 2538 (B—H), 1986, 1931 (MC≡O). ^{1}H NMR (ppm, CD_2Cl_2): 7.79–7.44 (envelope, 30 H, PPN), 7.09–6.87 (m, 5 H, –C$_6$H$_5$), 2.43 (s, 2 H, –MCH$_2$–), 1.91 (br s, 2 H, carborane C—H). ^{11}B{^{1}H} NMR (ppm, THF): −4.0, −7.1, −8.9, −11.1, −20.8, −23.2 (1:1:2:2:2:1).

[(CH$_3$)P(C$_6$H$_5$)$_3$][*closo*-3,3-(CO)$_2$-3-COCH$_3$-3,1,2-FeC$_2$B$_9$H$_{11}$] (6). To an orange solution of Na$_2$[**3**] (0.74 mmol) generated as described in the above general procedure was added 1 molar equiv of acetyl chloride (0.52 mL) by using a gastight syringe. An immediate color change to brownish yellow was observed. After the solvent was removed, the yellow residue was dissolved in 40 mL of acetonitrile and a solution of methyltriphenylphosphonium bromide (263 mg, 0.74 mmol) in 40 mL of CH_3CN was added. The

---

(19) Shriver, D. F. *The Manipulation of Air-Sensitive Compounds*; McGraw-Hill: New York, 1969.

(20) Gordon, A. J.; Ford, R. A. *The Chemist Companion*; Wiley: New York, 1972.

Table IV. Details of the Crystallographic Data Collection[a]

	$[N(C_2H_5)_4][\mathbf{7}]$	[PPN][**8**]	[PPN][**10**]
cryst size/mm	0.2 × 0.25 × 0.3	0.05 × 0.32 × 0.35	0.15 × 0.25 × 0.45
normal to faces	$\bar{1}10$, 001, 110	001, 010, 100	$0\bar{1}0$, $11\bar{1}$, $\bar{1}1\bar{1}$
appearance	orange parallelepiped	orange plate	amber parallelepiped (cut)
space group	$P\bar{1}$	$P2_1/m$	$P\bar{1}$
a/Å	11.209 (1)	9.1250 (7)	10.086 (4)
b/Å	13.026 (1)	25.011 (2)	15.390 (6)
c/Å	13.595 (1)	18.517 (2)	17.027 (7)
α/deg	79.959 (3)		112.636 (8)
β/deg	84.143 (3)	91.328 (2)	96.647 (8)
γ/deg	66.060 (2)		100.206 (9)
V/Å^3	1785	4225	2351
Z	2	4	2
ρ(calcd)/g cm^{-3}	1.35	1.25	1.20
μ/cm^{-1}	11.0 (not applied)	4.6	4.5
scan width			
below Kα_1	1.3	1.3	1.2
above Kα_2	1.6	1.6	1.6
scan rate/deg min^{-1}	4.5	6.0	6.0
no. of unique reflns	6302	8514	5761
no. of obsd ($I > 3\sigma(I)$) reflns	5572	3379	3272
2θ max/deg	50	52	44
data collcd	$+h, \pm k, \pm l$	$+h, +k, \pm l$	$+h, \pm k, \pm l$
no. of params refined	373	455	301
R, R_w, GOF	0.029, 0.042, 1.49	0.082, 0.095, 2.21	0.070, 0.078, 1.95

[a] Conditions: temperature/K, 298; radiation (graphite monochromator), Mo Kα; wavelength/Å, 0.7107.

solution was filtered over a Celite pad, the filtrate was reduced in volume, and addition of ether resulted in pale yellow microcrystals, which were dried under vacuum. Recrystallization from THF/heptane afforded 105 mg (25% yield) of analytically pure product. Anal. Calcd for $C_{25}H_{32}B_9O_3PFe$: C, 53.17; H, 5.72; B, 17.23; P, 5.48; Fe, 9.89. Found: C, 53.31; H, 5.63; B, 17.03; P, 5.61; Fe, 9.72. IR (cm^{-1}): 2558, 2521 (B—H), 1996, 1944 (MC≡O), 1582 (C=O). ^{1}H NMR (ppm, CD_2Cl_2): 7.93–7.53 (envelope, 15 H, $^+P(C_6H_5)_3$), 2.73 (d, 3 H, $^+P—CH_3$), 2.55 (s, 3 H, $-C(O)CH_3$), 2.51 (br s, 2 H, carborane C—H). $^{11}B\{^1H\}$ NMR (ppm, THF): −2.6, −6.9, −7.6, −10.4, −20.1, −22.6 (1:1:2:2:2:1).

$[N(C_2H_5)_4]$[*closo*-3,3-$(CO)_2$-3-$[Sn(C_6H_5)_3]$-3,1,2-$FeC_2B_9H_{11}$] (7). A solution of Na_2[3] (0.74 mmol) in THF was reacted with an equimolar slurry of triphenyltin chloride (283 mg) in 40 mL of THF. The solution was stirred at room temperature for 1 h, followed by removal of solvent. The orange residue was dissolved in 50 mL of acetonitrile, and 122 mg of tetraethylammonium chloride (0.74 mmol) in 50 mL of CH_3CN was added. After filtering through a Celite pad, the solution was reduced in volume and diethyl ether was added. The resulting orange crystals were collected and dried. Recrystallization from THF/Et_2O afforded 300 mg (56% yield) of analytically pure product. Anal. Calcd for $C_{30}H_{47}B_9NO_2FeSn$: C, 49.72; H, 6.41; B, 13.43; N, 1.94; Fe, 7.71; Sn, 16.38. Found: C, 49.57; H, 6.32; B, 13.23; N, 1.89; Fe, 7.61; Sn, 16.25. IR (cm^{-1}): 2577, 2562, 2546 (B—H), 1961, 1896 (MC≡O). ^{1}H NMR (ppm, CD_2Cl_2): 7.63–7.26 (m, 15 H, $-Sn(C_6H_5)_3$), 3.04 (q, 8 H, $^+N(-CH_2-)_4$), 2.75 (br s, 2 H, carborane C—H), 1.22 (t, 12 H, $(-CH_3)_4$). $^{11}B\{^1H\}$ NMR (ppm, THF): −1.4, −3.6, −9.0, −11.9, −20.4, −23.8 (1:1:2:2:2:1).

[PPN][*closo*-3-CO-3-(η^3-C_3H_5)-3,1,2-$FeC_2B_9H_{11}$] (8). A solution of Na_2[3], generated from 200 mg of 1 (0.74 mmol) and 2 equiv of sodium naphthalide as described in the general procedure, was stirred during the addition of an equimolar solution of allyl chloride (0.06 mL) in THF (40 mL). After filtration over a Celite pad, the orange solution was photolyzed for 18 h, followed by removal of solvent. The resultant orange residue was dissolved in 40 mL of acetonitrile, and PPN$^+$Cl$^-$ (450 mg, 0.78 mmol) in 40 mL of CH_3CN was added. The solution was filtered by using Celite followed by volume reduction. Upon addition of diethyl ether, reddish orange needles were collected and dried under vacuum. Recrystallization from THF/ether afforded 393 mg (67% yield) of analytically pure product. Anal. Calcd for $C_{43}H_{48}B_9NOP_2Fe$: C, 63.76; H, 5.99; B, 12.01; N, 1.73; P, 7.65; Fe, 6.90. Found: C, 63.56; H, 5.87; B, 11.76; N, 1.63; P, 7.76; Fe, 6.68. IR (cm^{-1}): 2544, 2518 (B—H), 1912 (MC≡O). ^{1}H NMR (ppm, CD_2Cl_2): 7.44–7.65 (envelope, 30 H, PPN), 3.96 (m, 1 H, H_c, $H_aH_sC—CH_c—CH_aH_s$), 2.62 (d, 2 H, H_s, $J_{H_s-H_c}$ = 7 Hz), 2.15 (br s, 2 H, carborane C—H), 1.15 (d, 2 H, H_a, $J_{H_a-H_c}$ = 11 Hz). $^{11}B\{^1H\}$ NMR (ppm, THF): −3.3, −7.9, −10.8, −13.5, −22.6, −26.3 (1:1:2:2:2:1).

[PPN][*closo*-3-CO-3-(η^3-C_4H_7)-3,1,2-$FeC_2B_9H_{11}$] (9). To a THF solution of Na_2[3] (0.74 mmol) was added an equimolar solution of methallyl chloride (0.073 mL) in 40 mL of THF. After filtering over a Celite pad, the orange solution was photolyzed for 18 h, followed by the removal of solvent. The resultant orange residue was dissolved in 40 mL of CH_3CN, and a solution of PPN$^+$Cl$^-$ (450 mg, 0.78 mmol) in CH_3CN (40 mL) was added. After filtration over a Celite pad, diethyl ether was added, resulting in the formation of light orange needles. Recrystallization from CH_3CN/Et_2O afforded 250 mg (44% yield) of analytically pure product. Anal. Calcd for $C_{47}H_{48}B_9NO_2P_2Fe$: C, 64.58; H, 5.55; B, 11.13; N, 1.60; P, 7.09; Fe, 6.39. Found: C, 64.49; H, 5.40; B, 11.12; N, 1.46; P, 7.21; Fe, 6.29. IR (cm^{-1}): 2534, 2507 (B—H), 1904 (MC≡O). ^{1}H NMR (ppm, CD_2Cl_2): 7.66–7.46 (envelope, 30 H, PPN), 2.30 (s, 2 H, H_s, $H_aH_sC—C(CH_3)—CH_aH_s$), 2.06 (br s, 2 H, carborane C—H), 1.84 (s, 3 H, $-CH_3$), 1.12 (s, 2 H, H_a). $^{11}B\{^1H\}$ NMR (ppm, THF): −3.9, −8.1, −11.2, −13.5, −22.8, −26.1 (1:1:2:2:2:1).

[PPN][*closo*-3-CO-3-$COCH_3$-3-$P(CH_3)_3$-3,1,2-$FeC_2B_9H_{11}$] (10). A 1 molar equiv sample of methyl iodide (0.045 mL) was added to an orange THF solution of Na_2[3] (0.074 mmol), resulting in an immediate color change to golden brown. The solution was allowed to stir at room temperature for 1 h, followed by the addition of 2.0 mL of $P(CH_3)_3$/THF (1.0 M, 2.0 mmol). The reaction was refluxed for 7 days. After removal of solvent, the yellow residue was dissolved in 40 mL of acetonitrile, and PPN$^+$Cl$^-$ (450 mg, 0.78 mmol) in CH_3CN (40 mL) was added. Filtration over a Celite pad was followed by reduction in volume and the addition of diethyl ether. The resultant bright yellow microcrystals were collected, dried under vacuum, and recrystallized from THF/Et_2O to afford 230 mg (39% yield) of analytically pure product. Anal. Calcd for $C_{44}H_{53}B_9NO_2P_3Fe$: C, 60.46; H, 6.12; B, 11.13; N, 1.60; P, 10.63; Fe, 6.39. Found: C, 60.46; H, 6.12; B, 10.63; N, 1.48; P, 10.63; Fe, 6.24. IR (cm^{-1}): 2529, 2519 (B—H), 1893 (MC≡O), 1564 (C=O). ^{1}H NMR (ppm, CD_2Cl_2): 7.66–7.44 (envelope, 30 H, PPN), 2.59 (s, 3 H, $-C(O)CH_3$), 2.08 (br s, 1 H, carborane (C—H), 1.92 (br s, 1 H, carborane C—H), 1.41 (d, 9 H, $P(CH_3)_3$, J_{P-H} = 9 Hz). $^{11}B\{^1H\}$ NMR (ppm, CH_3CN): −8.0, −10.7, −11.3, −13.8, −22.7, −23.3 (2:2:1:1:1:2).

Collection and Reduction of X-ray Data for $[N(C_2H_5)_4]$[7]. An orange crystal, obtained from a $CH_3CN/(C_2H_5)_2O$ solution, was mounted with epoxy on a fiber on a Huber diffractometer constructed by Professor C. E. Strouse of this department. Unit cell parameters were determined from a least-squares fit of 51 accurately centered reflections (9.4° < 2θ < 20.4°). These dimensions and other parameters, including conditions of data

Table V. Positional and Equivalent Isotropic Thermal Parameters for [N(C$_2$H$_5$)$_4$][7]^a

atom	x	y	z	$\langle U^2 \rangle$
Sn	0.197 11 (2)	0.641 04 (2)	0.271 69 (1)	0.037
Fe(3)	−0.042 14 (4)	0.667 28 (3)	0.283 00 (3)	0.039
O(3)	0.056 20 (23)	0.436 27 (18)	0.389 35 (19)	0.062
C(3)	0.021 29 (29)	0.528 02 (25)	0.347 09 (23)	0.045
O(4)	0.007 04 (34)	0.586 60 (30)	0.091 99 (22)	0.100
C(4)	−0.011 10 (37)	0.619 36 (32)	0.168 24 (27)	0.063
C(1)	−0.211 25 (29)	0.709 86 (25)	0.376 21 (24)	0.049
C(2)	−0.109 25 (29)	0.758 93 (23)	0.403 49 (22)	0.044
B(4)	−0.248 68 (36)	0.745 98 (31)	0.254 71 (30)	0.051
B(5)	−0.359 93 (38)	0.814 57 (35)	0.348 38 (36)	0.063
B(6)	−0.269 92 (38)	0.818 95 (32)	0.446 16 (31)	0.056
B(7)	−0.066 65 (33)	0.835 75 (27)	0.302 35 (25)	0.041
B(8)	−0.158 13 (35)	0.833 30 (29)	0.202 09 (26)	0.045
B(9)	−0.327 74 (37)	0.895 86 (33)	0.239 38 (33)	0.058
B(10)	−0.342 13 (39)	0.941 73 (32)	0.358 78 (34)	0.061
B(11)	−0.182 45 (38)	0.903 34 (29)	0.397 23 (29)	0.052
B(12)	−0.217 54 (36)	0.952 17 (29)	0.269 16 (29)	0.051
C(12)	0.166 46 (16)	0.835 69 (17)	0.092 45 (15)	0.053
C(13)	0.205 97 (16)	0.907 70 (17)	0.021 25 (15)	0.064
C(14)	0.332 86 (16)	0.902 45 (17)	0.020 56 (15)	0.068
C(15)	0.420 22 (16)	0.825 19 (17)	0.091 07 (15)	0.069
C(16)	0.380 70 (16)	0.753 18 (17)	0.162 27 (15)	0.056
C(11)	0.253 82 (16)	0.758 44 (17)	0.162 96 (15)	0.043
C(22)	0.360 53 (21)	0.378 53 (16)	0.298 07 (12)	0.051
C(23)	0.448 49 (21)	0.274 93 (16)	0.271 15 (12)	0.062
C(24)	0.503 80 (21)	0.269 89 (16)	0.174 50 (12)	0.076
C(25)	0.471 15 (21)	0.368 45 (16)	0.104 77 (12)	0.090
C(26)	0.383 19 (21)	0.472 05 (16)	0.131 69 (12)	0.073
C(21)	0.327 88 (21)	0.477 09 (16)	0.228 34 (12)	0.044
C(32)	0.240 98 (22)	0.564 71 (18)	0.497 56 (15)	0.060
C(33)	0.292 06 (22)	0.552 19 (18)	0.590 36 (15)	0.068
C(34)	0.363 87 (22)	0.614 49 (18)	0.603 30 (15)	0.075
C(35)	0.384 59 (22)	0.689 31 (18)	0.523 43 (15)	0.095
C(36)	0.333 51 (22)	0.701 84 (18)	0.430 63 (15)	0.071
C(31)	0.261 71 (22)	0.639 54 (18)	0.417 69 (15)	0.043

[a] Units of $\langle U^2 \rangle$ are Å^2. Units of each esd, in parentheses, are those of the least significant digit of the corresponding parameter. Isotropic values are $[1/(8\pi^2)]B_{eq}$.[24]

collection, are summarized in Table IV. Data were collected at 25 °C in the θ–2θ scan mode. Three intense reflections, (1,3,−2), (1,0,3), and (3,−2,−1), were monitored every 97 reflections to check stability. Intensities of these reflections fluctuated ca. ±5% with no decay during the course of the experiment (81.9 h). Of the 6302 unique reflections measured, 5572 were considered observed ($I > 3\sigma(I)$) and were used in the subsequent structure analysis. Data were corrected for Lorentz and polarization effects. Programs used in this work include locally modified versions of crystallographic programs listed in the reference section.[21]

Table VI. Positional and Equivalent Isotropic Thermal Parameters for [PPN][8]^a

atom	x	y	z	$\langle U^2 \rangle$
C(01)	0.0316 (11)	0.2829 (5)	0.2958 (7)	0.033 (7)
C(03)	0.3390 (19)	0.2500	0.4202 (10)	0.065 (12)
C(04)	0.0916 (17)	0.2016 (8)	0.4582 (9)	0.093 (13)
C(05)	0.0140 (29)	0.2500	0.4467 (16)	0.117 (24)
O(03)	0.4507 (13)	0.2500	0.4529 (6)	0.081 (9)
Fe(3)	0.1749 (3)	0.2500	0.3728 (1)	0.063 (2)
B(04)	0.2061 (14)	0.3067 (5)	0.2876 (8)	0.063 (9)
B(05)	0.0840 (17)	0.3045 (6)	0.2139 (10)	0.081 (11)
B(06)	−0.0295 (27)	0.2500	0.2200 (14)	0.101 (20)
B(08)	0.3242 (19)	0.2500	0.2842 (9)	0.077 (13)
B(09)	0.2678 (17)	0.2854 (6)	0.2034 (8)	0.118 (13)
B(10)	0.1159 (30)	0.2500	0.1613 (12)	0.129 (23)

[a] Units of $\langle U^2 \rangle$ are Å^2. Units of each esd, in parentheses, are those of the least significant digit of the corresponding parameter. Isotropic values are $[1/(8\pi^2)]B_{eq}$.[24] A more complete list of parameters is included with the supplementary material.

Table VII. Positional and Equivalent Isotropic Thermal Parameters for [PPN][10]^a

atom	x	y	z	$\langle U^2 \rangle$
Fe(3)	0.70894 (13)	0.608 23 (10)	0.219 88 (8)	0.0411 (8)
C(01)	0.73266 (91)	0.758 49 (62)	0.275 58 (58)	0.0536 (63)
C(02)	0.59013 (90)	0.701 54 (67)	0.203 57 (58)	0.0490 (60)
B(04)	0.7452 (10)	0.712 50 (78)	0.352 41 (65)	0.0463 (68)
B(05)	0.7027 (11)	0.827 37 (84)	0.375 00 (69)	0.0556 (76)
B(06)	0.6027 (12)	0.818 80 (83)	0.277 09 (76)	0.0718 (87)
B(07)	0.5002 (10)	0.616 94 (80)	0.227 17 (68)	0.0399 (67)
B(08)	0.5953 (10)	0.623 37 (80)	0.325 51 (66)	0.0433 (67)
B(09)	0.6090 (11)	0.740 60 (82)	0.405 44 (67)	0.0526 (73)
B(10)	0.5209 (12)	0.806 63 (81)	0.359 90 (70)	0.0760 (86)
B(11)	0.4539 (11)	0.728 25 (83)	0.249 17 (68)	0.0466 (69)
B(12)	0.4554 (11)	0.679 19 (83)	0.327 62 (69)	0.0449 (68)
C(13)	0.6385 (10)	0.482 28 (83)	0.171 01 (67)	0.0521 (70)
O(13)	0.58918 (80)	0.405 36 (55)	0.143 06 (54)	0.0878 (62)
O(14)	0.85176 (88)	0.678 34 (64)	0.118 72 (49)	0.1200 (72)
C(14)	0.7707 (10)	0.607 66 (84)	0.113 88 (86)	0.0440 (66)
C(15)	0.7230 (14)	0.537 1 (10)	0.031 43 (73)	0.1400 (13)
P(01)	0.91180 (27)	0.586 09 (21)	0.255 53 (17)	0.0495 (17)
C(16)	0.9689 (13)	0.495 35 (93)	0.170 43 (68)	0.0955 (93)
C(17)	1.05350 (95)	0.692 44 (81)	0.290 03 (78)	0.0340 (64)
C(18)	0.9286 (11)	0.541 69 (79)	0.340 13 (67)	0.0844 (82)

[a] Units of $\langle U^2 \rangle$ are Å^2. Units of each esd, in parentheses, are those of the least significant digit of the corresponding parameter. Isotropic values are $[1/(8\pi^2)]B_{eq}$.[24]

Solution and Refinement of the Structure of [N(C$_2$H$_5$)$_4$][7]. Atoms were located by use of statistical methods (SHELX86).[21] All calculations were performed on the VAX 3100 crystallographic computer. All methyl and phenyl hydrogens were included in calculated positions as members of rigid groups, C–H = 1.0 Å, H–C–H = 109.5° and C–C = 1.395 Å, C–H = 1.0 Å, angles = 120°, respectively. The other hydrogens of the cation were also included in calculated positions. Position parameters for carboranyl hydrogens were included in located positions. H atoms were assigned u values of 0.12, 0.10, 0.08, and 0.04 Å^2 for methyl, methylene, phenyl, and carboranyl hydrogens, respectively. Scattering factors for hydrogen were obtained from Stewart et al.[22] and for other atoms were taken from ref 23. Anomalous dispersion terms were applied to the scattering of Fe. The largest peak on a final difference electron density map was 0.5 e Å^{-3}. Final positional and thermal parameters for non-hydrogen atoms are given in Table V.

Collection and Reduction of X-ray Data for [PPN][8]. An orange crystal, obtained from a CH$_3$CN/(C$_2$H$_5$)$_2$O solution, was mounted with epoxy on a thin glass fiber on a modified Huber diffractometer. Systematic absences were found for 0*k*0 reflections for which $k \neq 2n$. Unit cell parameters were determined from a least-squares fit of 49 accurately centered reflections (9.4° < 2θ < 20.0°). These dimensions and other parameters, including conditions of data collection, are summarized in Table IV. Data were collected at 25 °C in the θ–2θ scan mode. Three intense reflections, (0,3,−4), (0,3,4), and (2,2,0), were monitored every 97 reflections to check stability. Intensities of these reflections did not decay during the course of the experiment (90.7 h, fluctuation 10%). Of the 8514 unique reflections measured, 3379 were considered observed ($I > 3\sigma(I)$) and were used in the subsequent structure analysis. Data were corrected for Lorentz and polarization effects. Programs used include locally modified versions of the crystallographic programs listed in the reference section.[21]

Solution and Refinement of the Structure of [PPN][8]. Atoms were located by use of the heavy-atom method. All calculations were performed on the VAX 3100 crystallographic computer. All phenyl hydrogens were included in calculated positions as members of rigid groups, C–H = 1.0 Å, angles = 120°. All carboranyl hydrogens were kept in located positions. Hydrogen

---

(21) CARESS (Broach, Coppens, Becker, and Blessing), peak profile analysis, Lorentz and polarization corrections; ORFLS (Busing, Martin, and Levy) structure factor calculation and full-matrix least-squares refinement; ABSORB (Coppens, Edwards, and Hamilton), absorption correction calculation; SHELX86 and SHELX76 (Sheldrick), structure analysis package; ORTEP (Johnson), figure plotting.

(22) Stewart, R. F.; Davidson, E. R.; Simpson, W. T. *J. Chem. Phys.* **1965**, *42*, 3175.

(23) *International Tables for X-ray Crystallography*; Kynoch Press: Birmingham, England, 1974; Vol. IV.

(24) Hamilton, W. C. *Acta Crystallogr.* **1959**, *12*, 609.

atoms were assigned u values of 0.07 Å^{-3}. Scattering factors for hydrogen were obtained from Stewart et al.[22] and for other atoms were taken from ref 23. Anomalous dispersion terms were applied to the scattering of Fe and P. The largest peak on a final difference electron density map was ±0.5 e Å^{-3}. Final positional and thermal parameters for non-hydrogen atoms are given in Table VI.

Collection and Reduction of X-ray Data for [PPN][10]. An amber crystal, obtained from a $(CH_2)_4O/C_2H_5)_2O$ solution, was mounted with epoxy on a thin glass fiber on a modified Huber diffractometer. Unit cell parameters were determined from a least-squares fit of 25 accurately centered reflections ($9.5° < 2\theta < 16.4°$). These dimensions and other parameters, including conditions of data collection, are summarized in Table IV. Data were collected at 25 °C in the θ–2θ scan mode. Three intense reflections, (2,–1,4), (0,3,3), and (3,1,–3), were monitored every 97 reflections to check stability. Intensities of these reflections decayed less than 1% with a maximum fluctuation of ±4.7% during the course of the experiment (55.2 h). Of the 5761 unique reflections measured, 3272 were considered observed ($I > 3\sigma(I)$) and were used in the subsequent structure analysis. Data were corrected for Lorentz and polarization effects. Programs used include locally modified versions of the programs listed in the reference section.[21]

Solution and Refinement of the Structure of [PPN][10]. Atoms were located by use of the heavy-atom method. All calculations were performed on the VAX 3100 crystallographic computer. All phenyl hydrogens were included in calculated positions as members of rigid groups, C–H = 1.0 Å, angles = 120°. All methyl hydrogens were included in calculated positions, C–H = 1.0 Å, H–C–H = 109.5°. All carboranyl hydrogens were kept in located positions. Hydrogen atoms were assigned u values based on those of the attached atoms. Scattering factors for hydrogen were obtained from Stewart et al.[22] and for other atoms were taken from ref 23. Anomalous dispersion terms were applied to the scattering of Fe and P. The largest peak on a final difference electron density map was 0.6 e Å^{-3} and was located near a phenyl ring. Final positional and thermal parameters for nonhydrogen atoms are given in Table VII.

Acknowledgment. We gratefully acknowledge financial support provided by the Office of Naval Research.

Supplementary Material Available: Tables of positional and thermal parameters, anisotropic thermal parameters, and interatomic distances and angles (29 pages); listings of observed and calculated structure factors (70 pages). Ordering information is given on any current masthead page.

Synthesis and Kinetics of Decomposition of Tungsten(VI) and Molybdenum(VI) 2-Oxametallacyclobutane Complexes and the X-ray Structure of *trans*-Mo[CH(*t*-Bu)CH(C_6F_5)O](NAr)(O-*t*-Bu)$_2$

Guillermo C. Bazan, Richard R. Schrock,* and Marie B. O'Regan

Department of Chemistry 6-331, Massachusetts Institute of Technology, Cambridge, Massachusetts 02139

Received July 13, 1990

2-Oxametallacyclobutane complexes (M = Mo (**2a**), W (**2b**)) can be prepared by adding pentafluorobenzaldehyde to M(CH-*t*-Bu)(NAr)(O-*t*-Bu)$_2$ (M = Mo (**1a**), W (**1b**)). Two isomers are observed for **2a** and **2b** that contain *t*-Bu and Ph_F substituents trans or cis to one another (the trans isomer predominating) and that decompose to give *trans*- or *cis*-Ph_FCH=CH(*t*-Bu), respectively. An X-ray structure of the major isomer of **2a** (**2a**-trans) showed it to be a square pyramid containing an apical imido ligand and pseudoequatorial α-*t*-Bu and β-Ph_F groups in a slightly puckered $MoOC_2$ ring. It is proposed that cis isomers of **2** also contain a pseudoequatorial α-*t*-Bu group. At 25 °C **2a**-trans decomposes twice as rapidly as **2b**-trans, and at 5.0 °C **2b**-cis decomposes ~25 times more rapidly than **2b**-trans. These findings are all consistent with square-pyramidal 2-oxametallacyclobutane complexes being more stable when they contain trans α and β substituents, when electron-withdrawing substituents are present on the ring, and when a bulky substituent is present in the pseudoequatorial α position. These results are discussed in relation to findings concerning analogous MC_3 metallacyclobutane complexes.

Introduction

2-Oxametallacyclobutane (metallaoxetane) complexes are plausible intermediates in transition-metal-catalyzed olefin epoxidation reactions[1] and Wittig-like reactions between high oxidation state alkylidene complexes and the carbonyl functionality.[2,3] However, examples usually can be prepared only by indirect methods.[4] An exception in

---

(1) (a) Collman, J. P.; Brauman, J. L.; Meunier, B.; Hayashi, T.; Kodadek, T.; Raybuck, S. A. *J. Am. Chem. Soc.* **1985**, *107*, 2000. (b) Groves, J. T.; Avaria-Neisser, G. E.; Fish, K. M.; Imachi, M.; Kuczkowski, R. L. *J. Am. Chem. Soc* **1986**, *108*, 3837. (c) Sharpless, K. B.; Teranishi, A. Y.; Bäckvall, J.-E. *J. Am. Chem. Soc.* **1977**, *99*, 3120. (d) Milstein, D.; Calabrese, J. C. *J. Am. Chem. Soc.* **1982**, *104*, 3773. (e) Alper, H.; Arzoumanian, H.; Petrignani, J.-P.; Saldana-Maldonado, M. *J. Chem. Soc., Chem. Commun.* **1985**, *340*. (f) Girardet, M.; Meunier, B. *Tetrahedron Lett.* **1987**, 2955. (g) Mock, W. L.; Bieniarz, C. *Organometallics* **1985**, *4*, 1917. (h) Walba, D. M.; DePuy, C. H.; Grabowski, J. J.; Bierbaum, V. M. *Organometallics* **1984**, *3*, 498.

(2) (a) Schrock, R. R. *J. Am. Chem. Soc.* **1976**, *98*, 5399. (b) Tebbe, F. N.; Parshall, G. W.; Reddy, G. S. *J. Am. Chem. Soc.* **1978**, *101*, 3611. (c) Pines, S. H.; Zahler, R.; Evans, D. A.; Grubbs, R. H. *J. Am. Chem. Soc.* **1980**, *102*, 3270. (d) Buchwald, S. L.; Grubbs, R. H. *J. Am. Chem. Soc.* **1983**, *105*, 5490. (e) Aguero, A.; Kress, J.; Osborn, J. A. *J. Chem. Soc., Chem. Commun.* **1986**, 531.

(3) (a) 3-Oxaplatinacyclobutane complexes have been reported.[3b] So far there is no evidence that 3-heteroatom metallacycles are formed in reactions between alkylidene complexes and the carbonyl function. (b) Hoover, J. F.; Stryker, J. M. *J. Am. Chem. Soc.* **1989**, *111*, 6466.

0276-7333/91/2310-1062$02.50/0